EMISSION CURRENT FLUCTUATIONS VS BEAM LIGHTNING OF THE FIELD-EMISSION CATHODE

Alexandr Knápek

Doctoral Degree Programme (4), FEEC BUT

E-mail: xknape03@stud.feec.vutbr.cz

Supervised by: Lubomír Grmela

E-mail: grmela@feec.vutbr.cz

Abstract: Paper deals with noise diagnostics which was performed on the cold field emission cathode in high-vacuum conditions (HV). Used cold field-emission cathode is designed to be used in low-voltage TEM, and is based on tungsten cathode with ultra-sharp nano-tip. The cathode is additionally coated by epoxy resin to stabilize the emission current, providing small and stable source of electrons. Technological issues are further examined by the means of the noise diagnostics, which provides information about carrier transport and cathode performance in general. The analysis was performed both in time and frequency domain. Mutual correlation between the current noise spectral-density, extractor voltage, beam brightness and Allan dispersion were analyzed, together with the main sources of noise.

Keywords: field emission stability, tungsten cathodes, Allan dispersion

1. INTRODUCTION

Among all the types of electron emission, the cold-field emission is becoming the predominant electron source for devices using focused electron beam, such as the modern low-energy transmission electron microscopes (TEM). Low energy TEMs (until 10 kV) are mostly intended to work with specimens sensitive to the radiation damage (these could be for instance biological samples – pathogens, tissues or even DNA molecules). Apart from avoiding the radiation damage, working with cold field emission source poses the possibility of working directly with the virtual source, which reduces number of electron optics used and simplifies the TEM construction. The only disadvantage, which remains, is the significant own noise, which reduces performance and resolution of the TEM. Further in the text, the relation between the technology parameters (structure of the surface layers) and current fluctuation is examined.

The experimental set-up consists of a DC source, intended both for powering the electron jet (acceleration and extractor voltage) and both for powering up ion pump, which is used for the second-stage chamber's decompression. Measured signal that is in fact the current measured on the scintillation screen. The current is then pre-amplified and further sampled in to the PC. For the experimental setup, it is necessary to work, at least, under the High Vacuum (HV), when the pressure is lower or equal than 1×10^{-6} Pa. Such a low pressure is reached by combined means of turbo-molecular and ion-pump. Ultra low pressure is needed: to reduce amount of ion-particles in the chamber, which tends to being attracted back to the cathode's surface and to bombard its surface while damaging the epoxy layer or the tip itself, to protect against the high-voltage, which could cause discharge (voltage surge) between the extractor and the cathode, that is very dangerous and could seriously damage equipment and cathode itself, the gas molecules could been absorbed on the cathode surface, that would lower the cathode current.

2. MATERIAL ANALYSIS

The width of the oxide layer was measured by the ionic etching method. The method is based on creating a steep sided hole in tungsten, which is then ripped-off . Extracted lamella is then analyzed (as you can see on fig. 1.a) by the means of transmission electron microscope equipped with *Gatan image filter* which allows the energy filtering of images (fig. 1.b). According to our observations, the oxide layer possess approximately 10 nm thick homogeneous-layer covering surface of the emission plane, which is located on the cathodes' tip. Taking into account oxide materials in general are chemically inert, robust, and have a relatively high melting temperature, it can be concluded that they stabilize the current even in lower vacuum conditions.

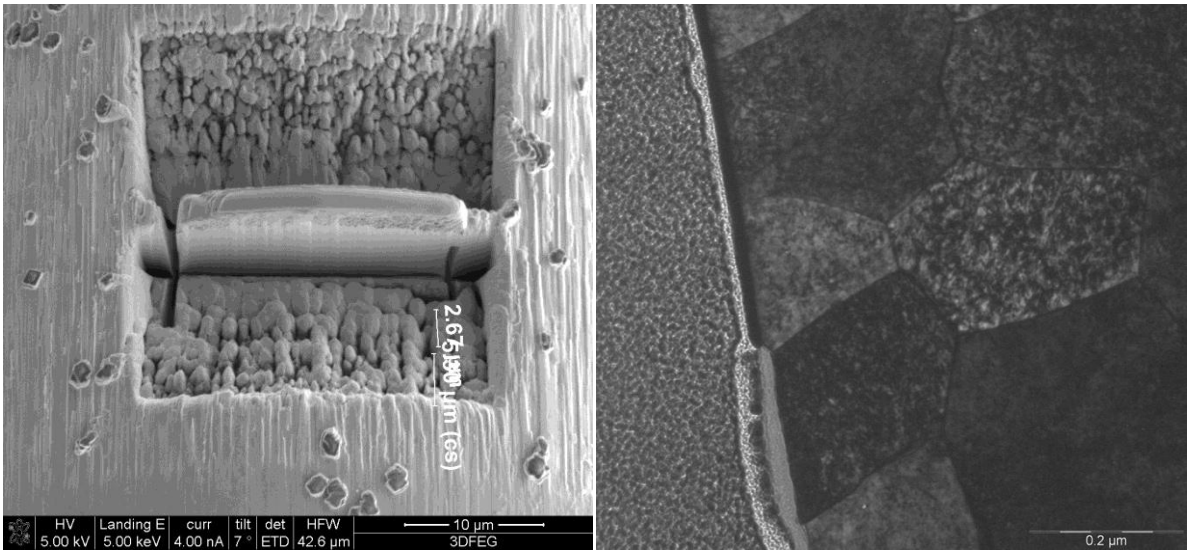

Figure 1: a) surface saw-cut b) sectional area of the oxide layer showing its width

Fluctuation occurrence is not influenced only by the compactness and purity of the oxide layer; also the thickness has essential impact on to the tunneling-current stability. Tungsten wire often suffers from surface contamination, which is caused due to the presence of carbon affecting the work function and can also causing current fluctuations. Therefore the oxide layer also directly influences the threshold field, while decreasing its intensity. Mathematically, the problem can be illustrated using *Fowler-Nordheim* (F-N) equation

$$\mathrm{j} = \frac{\mathrm{aA}\beta^2\mathrm{E}^2}{\varphi}\exp\left(\frac{-\mathrm{b}\varphi^{\frac{3}{2}}}{\beta\mathrm{E}}\right), \tag{1}$$

where *a* and *b* are constants, *A* is the emission area, *b* is the enhancement factor, *E* is the applied electric field and *j* is the work function. Local electric field of the emitter tip (E_1) is related to the β and the macroscopic field (E_m) by $E_1 = \beta E_m$ where the resulting current is equal to [2]

$$\mathrm{I} = \beta \cdot \mathrm{j}. \tag{2}$$

The field enhancement factor is essential while computing emission current and can be calculated from the slope of the *F-N plot* ($\ln I = V^2$ vs $I = V$), where *j* is equal to 5.59 -5.7 eV [3], according to the work function of the WO_3. The calculated β value of the oxide-covered sharp tip, considering the hemiellipsoid plane geometry given by [2]

$$\beta = \frac{\zeta^3}{\nu\cdot\ln(\nu+\zeta)-\zeta}, \zeta = (\nu^2-1)^{1/2}, \nu = \frac{\mathrm{L}}{\rho}, \tag{3}$$

where *z* is the numerator term, *L* stands for the semi-major axis length and *r* is the semi-minor axis length (see fig. 2). For the virgin tungsten field-emitter the *b* can be computed using more analytic from, that is given by [2] where *l*, *r* are the length and radius of the cathode tip, *L* is the tip length and *R* is the radius of the electrochemically sharpened tungsten tip and *D* is the distance between the electrodes. Smith [5] also suggests that by resin coated cathode, the emission current is limited by the supply of carriers to the surface, which strictly depends on the applied potential up to the spastic rise of the carrier concentration.

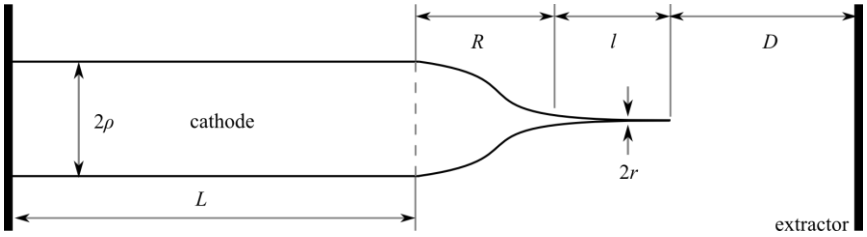

Figure 2: Scheme of an ideal C.F.E. cathode with ultra-sharp tip

3. RELATIVE LIGHT INTESITY

Together with the noise diagnostics, correlation between the extractor voltage and relative lightning intensity was examined. The lightning intensity have been measured in relative ratio, for which we have used the luminance intensity given by the *HSL* (L=luminance) model. The luminance level (beam lightning) was obtained from the central maximum, created by the incident electron beam on to the YAG crystal. Exact diameter of the area covered by the electron beam and its aura, was approximated as well (see fig. 3).

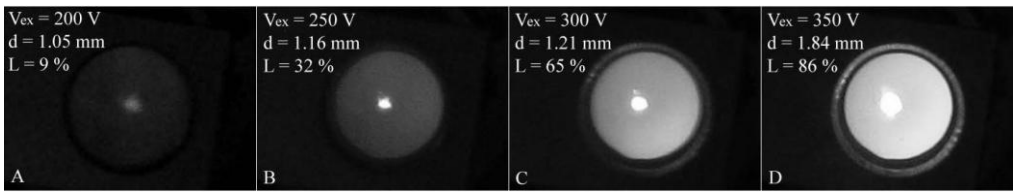

Figure 3: Cathode emission patterns for various extraction voltages

This information is important also for computing the cathode brightness, which is one of the essential parameters used for cathode characterization. Photographs of the incident plane of the YAG scintillator are illustrated in the fig. 3. Using the outcome from equations 1, 2 and 3, we are now able to determine the cathode brightness mentioned earlier in the text, according to the very well know formula

$$B = \frac{j}{\pi\alpha^2}\ [A \cdot m^{-2} \cdot sr\text{-}1] \qquad (4)$$

where a is the angle of divergence, of the electron beam. Taking into account that the emitting area is getting lower as the tip diameter is getting thick, the electron beam brightness is also rising. This also means that the cold emission cathode is brighter in comparison with the thermo-emission one.

4. INSTABILITY EVALUATION IN TIME DOMAIN

Allan dispersion has been used for the instability evaluation. Whole process was performed using computer script, which worked with a finite number of samples y_k. From this reason, it was necessary to obtain an estimate $\sigma^2_y(t)$, that unavoidably caused some statistical indeterminacy. In practice, *Allan* dispersion is implemented using the expression [6]

$$\sigma_{\bar{y}}^2(\tau, m) = \frac{1}{2(m-1)} \sum_{i=1}^{m-1} (\bar{y}_{i+1} - \bar{y}_i)^2, \qquad (5)$$

after which a curve was plotted for the function $\sigma_y(\tau)$ versus τ(s), see fig 4. The simplicity of the dependence of σ_y on t is considered to be one of the biggest advantages for the noise studies. If the spectral density of the fluctuations is proportional to white noise f^{-1} (flickering noise), or f^{-2} (G-R noise), then σ_y varies correspondingly in proportion to $\tau^{-1.5}$, τ^0 and $\tau^{1.5}$. Therefore, it is possible to draw particular conclusions about the nature of the noise, according to the function $\sigma_y(\tau)$.

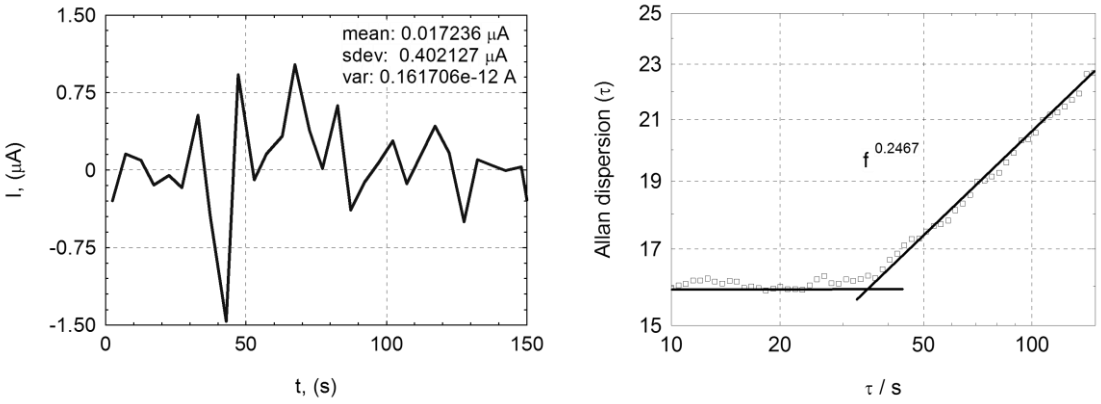

Figure 4: a) Emission current in time domain b) The corresponding Allan dispersion

5. NOISE ANALYSIS IN FREQUENCY DOMAIN

The results of the noise diagnostics, performed in time domain (fig. 4.a), are further supported by the spectral analysis. According to the fig. 5.a it can be seen, that the power spectral density of whole spectra is being slowly increased in time, and that the slope is staying constant. From the slope, which is constantly about $f^{1.5}$, it is evident that measured noise has characteristics of so called 1/*f* (flickering) noise.

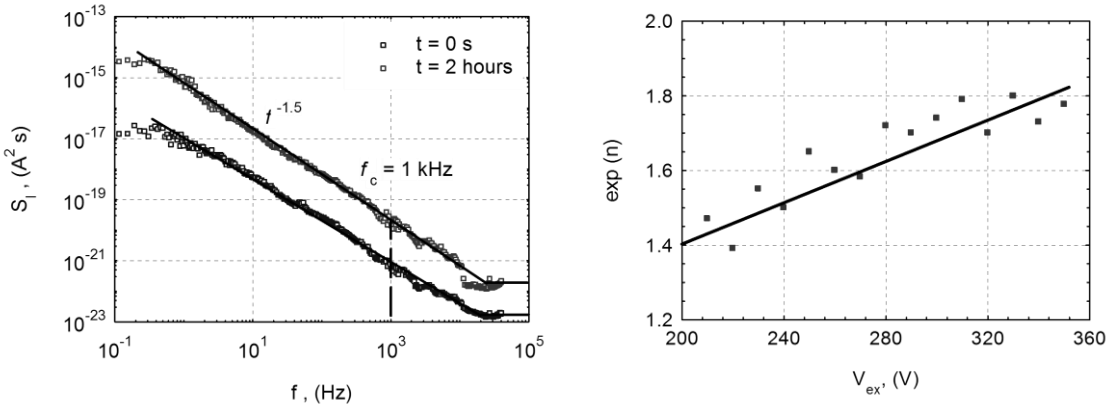

Figure 5: a) Emission current spectral noise analysis b) Noise spectrum slope vs. V_{ex}

In the second experiment (see fig. 5.b), the function of extractor voltage, which slowly changes, have been observed. According to measured data the noise spectrum is most significant around the V_{ext} = 260 V and 340 V, thus the lowest fluctuations were observed around V_{ext} = 300 V.

6. CONCLUSIONS

Cathode structure has been deeply examined and described. Obtained results suggest that the quality of the oxide layer has major impact on the charge carrier transport and electric threshold field. Charge carrier concentration significantly increases the electric field intensity and affects electron beam brightness as well. The presence of residual ions (present in the vacuum chamber) was observed from the noise measurements. As the ions hits the cathode surface, so called *burst noise* becomes more evident and can be easily observed in the time domain. The bombardment reduces the epoxy layer and thus destabilizes the emission current, which is illustrated also by the function of the Allan dispersion in time.

In the frequency domain, the main sources of the electric noise were mainly the generation-recombination processes, the $1/f$ noise and the thermal noise. The noise spectral density of the emission current, is mainly influenced by the $1/f^{n}$ noise, where n is located between 1 and 2. The $1/f^{n}$ noise originates from the superposition of particular generation-recombination (G-R) processes, therefore the higher the n is, the more significant G-R appears.

Correlation between the beam light intensity and extractor voltage has been examined as well. It has been discovered, that the optimal relation between noise fluctuation level, the light intensity and extractor voltage is around the V_{ext} = 300 V. The cold field-emission cathode is brighter in comparison to the thermoemission cathode, which allows reaching higher current density for the beams of the sub-micron diameter. For these reasons, cold field emission cathodes are more suitable for the purpose of TEM.

ACKNOWLEDGEMENT

This research has been partially supported by european project EU CZ.1.05/2.1.00/03.0072 „*Centre for sensor, information and communication systems*“ (SIX) and by operation programme for science and competitiveness CZ.1.07/2.2.00/15.0147 „*The nano-science for engineering – innovation of study programs*“ (Nanosciences).

REFERENCES

[1] YU, Z. Q., et al., Reproducible tip fabrication and cleaning for UHV STM. *Ultramicroscopy* (online). 2008, s. 873-877.

[2] FORBES, R. G., EDGCOMBE, C. J., VALDRE, U., *Ultramicroscopy* 95, p. 57

[3] RAGHUNANDAN, S., JUN, H., JUCHEOL, P., DONG, H. K., WON, B. C., Multistage field enhancement of tungsten oxide nanowires and its field emission in various vacuum conditions, *Nanotechnology* 17 (2006), 4840-4844.

[4] SLAIDINŠ, I., Accuracy of Noise Measurements for 1/f and GR Noise, Advanced Experimental Methods For Noise Research in *Nanoscale Electronic Devices*, vol. 151, 271-278, Springer 978-1-4020-2169-5, ISBN: 978-1-4020-2169-5.

[5] SMITH, R. C., et al., *Appl. Phys. Lett.*, 2005, 87 0143111

[6] KANDA, M., IEEE Trans. Microwave Theory Tech., MTT-25, August 676-82 (1977).